Journal Pre-proof

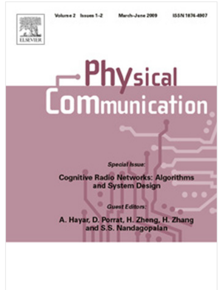

An improved indoor positioning based on crowd-sensing data fusion and particle filter

Ahmed Gamal Abdellatif, Amgad A. Salama, Hamed S. Zied, Adham A. Elmahallawy, Mahmoud A. Shawky

PII: S1874-4907(23)00228-8
DOI: https://doi.org/10.1016/j.phycom.2023.102225
Reference: PHYCOM 102225

To appear in: *Physical Communication*

Received date : 29 May 2023
Revised date : 26 October 2023
Accepted date : 3 November 2023

An Improved Indoor Positioning based on Crowd-Sensing Data Fusion and Particle Filter

Ahmed Gamal Abdellatif[a,*], Amgad A. Salama [b], Hamed S. Zied[a], Adham A. Elmahallawy[c] and Mahmoud A. Shawky[d,*]

[a] Department of Electronics and Electrical Communications Engineering, Air Defence Collage, Alexandria, Egypt
[b] The Research and Development Center, Air Defence Collage, Cairo, Egypt
[c] Higher institute of Engineering and Technology, king Mariout, Alexandria, Egypt
[d] James Watt School of Engineering, University of Glasgow, G12 8QQ, Glasgow, UK

ARTICLE INFO

Keywords:
Inertial measurement unit
Particle filter
Pedestrian dead reckoning
Received signal strength
Ultra-wideband

ABSTRACT

Due to the lack of global positioning system (GPS) signals in some enclosed areas, indoor localization has recently gained significant importance for academics. However, indoor localization has a number of challenges and defects, including accuracy, cost, coverage, and ease of use. This paper explores the integration between the inertial measurement unit (IMU) and Wi-Fi-based received signal strength indicator (RSSI) measurements, demonstrating their combined potential for robust indoor localization. IMUs excel at capturing precise short-term motion dynamics, offering insights into an object's acceleration and orientation. Conversely, RSSI measurements serve as valuable indicators for relative positioning within indoor environments. By fusing data from these sources, our approach compensates for the inherent weaknesses of each sensor type. To achieve accurate indoor positioning, we employ techniques such as sensor fusion, Wi-Fi fingerprinting, and dead reckoning. Wi-Fi fingerprinting allows us to create a database that maps RSSI measurements to specific locations, while dead reckoning helps mitigate drift and inaccuracies. By combining these methods, we estimate a device's position with increased precision. Through experimental evaluation, we assess the performance and efficiency of our integrated approach, comparing the estimated path or new location with a predefined reference path. The findings emphasise a significant improvement in accuracy, with the integration of crowd-sensing, particle filtering, and magnetic fingerprinting techniques resulting in a notable increase from 80.49% to 96.32% accuracy.

1. Introduction

Indoor localization systems offer a wide range of applications and services, primarily focused on the identification and monitoring of individuals through the wireless signals emitted by their personal devices, as well as the utilisation of wireless sensor networks for asset tracking. The advent of the internet-of-things (IoT) has introduced a pivotal application in this domain, enabling seamless connectivity and communication within smart homes, hospitals, schools, malls, and factories by leveraging various IoT technologies such as SigFox, LoRa, Wi-Fi HaLow, Weightless, and NB-IoT. Additionally, other wireless standards including BLE, Wi-Fi, Zigbee, RFID, and UWB play a significant role in facilitating these functionalities [1]. However, the development of an indoor localization system that achieves high accuracy, flexibility, affordability, and user-friendliness presents significant challenges [2, 4]. In this challenging scenario, relying on a single sensor for indoor localization is not recommended, as it leads to cumulative errors over time and inaccurate positioning [4]. Therefore, the integration of multiple sensors becomes necessary for computing predicted paths or determining new locations. This involves aggregating and synchronizing data and information from different sensors and feeding them into an estimation algorithm. Comparisons between the estimated path or new location and a predefined reference path are performed to assess the performance and efficiency of the proposed method.

Designing an indoor localization system with the aforementioned characteristics requires careful consideration and innovative approaches to address the challenges associated with accuracy, flexibility, cost-effectiveness, and usability [5]. The proposed method aims to overcome these challenges and demonstrate superior performance and efficiency compared to existing approaches. This paper introduces an enhanced indoor localization system that utilises a particle filter algorithm and incorporates crowd-sensing or multi-sensor fusion techniques. The aim is to achieve a low-cost system that maintains high accuracy and robustness. The proposed system combines traditional positioning technologies with innovative approaches to overcome limitations and improve performance.

Our proposed system aims to enhance the accuracy of indoor positioning by leveraging a combination of technologies. It integrates inertial navigation, utilising data from an inertial measurement unit (IMU), with a prior training phase and a carefully constructed magnetic map created using fingerprinting techniques. This integration serves to mitigate the inherent drift-related inaccuracies associated with IMU-based systems. Additionally, our system utilises the pedestrian dead reckoning (PDR) method [6], which allows for

* Corresponding author.
ag.abdellatef@zu.edu.eg (A.G. Abdellatif); amgad.A.salama@acm.org (A.A.S.); Dr.Hamed_zied@gmail.com (Hamed S. Zied); adhamegypt0@gmail.com (A.A. Elmahallawy); m.shawky.1@research.gla.ac.uk (M.A. Shawky)
ORCID(s): 0000-0002-3440-8448 (A.G. Abdellatif)

unrestricted data collection. To determine the user's position accurately, our positioning algorithm takes into account two data sources: the magnetic field and received signal strength (RSS) data from Wi-Fi devices [7, 8]. These data are compared to a fingerprint map database that has been pre-established. This comprehensive approach offers a robust solution for predicting the user's movements within a defined test area. By combining IMU data, PDR, and magnetic field or RSS data with a fingerprint map, the system minimises positioning errors and provides reliable indoor localization.

The system constructs a magnetic fingerprint database specific to the test area by fusing all available data and feeding it into the particle filter algorithm. The positioning results are promptly transmitted to the server, enabling real-time responsiveness to dynamic changes within the test area. To prove the validation of the proposed method, ultra-wideband (UWB) anchors are utilised to compute the reference trajectory, which closely approximates the actual path of the user equipment (UE). This reference trajectory is computed using the trilateration method and then compared with the predicted trajectory computed by the particle filter, demonstrating the effectiveness of the proposed technique.

The proposed framework offers several significant contributions, which can be summarised as follows:

1. The proposed framework provides a comprehensive exploration and analysis of various techniques, methods, technologies, and algorithms employed in indoor positioning. Through an extensive evaluation and comparison, it offers a profound understanding of the effectiveness and performance of different positioning methods and algorithms. This in-depth analysis serves as a valuable resource for researchers in the field, providing them with valuable insights that can drive innovation and the development of more accurate algorithms to meet the evolving requirements of indoor positioning in the future.
2. The proposed approach introduces a cost-effective mobile mapping and reliable indoor positioning system that combines crowd-sensing data fusion with a particle filter. It utilises fingerprinting to incrementally construct a comprehensive database for the test area, employing an infrastructure-free or PDR method to collect data and determine Wi-Fi device-equipped region's RSS values. For accurate performance evaluation, the positions of deployed UWB devices are leveraged for trilateration-based trajectory computation of the UE, which is then compared to the estimated trajectory using the proposed approach.
3. Finally, this paper employs a particle filter algorithm to enhance indoor localization accuracy through the fusion of data from various sources, including Wi-Fi, RSS, magnetic field measurements, UWB, and smartphone inertial sensors (i.e., IMUs). synchronizing the Wi-Fi access points with particles posed a challenge in achieving high granularity and precise timing. The findings presented in this paper demonstrate the remarkable capability of the proposed system to significantly improve performance. The results indicate an enhancement from 80.49% to 96.32% accuracy by integrating crowd-sensing, particle filtering, and magnetic fingerprinting techniques.

Table 1
List of Acronyms.

Symbol	Definition
AOA	Angle of arrival
CSI	Channel state information
IMU	Inertial measurement unit
IoT	Internet-of-things
NICs	Network interface cards
PDF	Probability density function
PDR	Pedestrian dead reckoning
PF	Particle filter
PoA	Phase of arrival
RNs	Reference nodes
RSS	Received signal strength
RSSI	Received signal strength indicator
RToF	Return time of flight
TDoA	Time difference of arrival
ToF	Time of flight
UWB	Ultra-wideband

For ease of understanding, the acronyms used in this paper are listed in Table 1.

This paper is organised into the following sections: Section 2 discusses related work. Section 3 covers preliminary concepts, providing a foundation for the subsequent sections. Section 4 presents the system and scheme modelling. Section 5 presents and discusses the experimental results. Lastly, Section 6 provides the conclusions.

2. Related Works

This paper specifically examines the utilisation of Wi-Fi technology based on the RSS fingerprinting technique for indoor positioning. In this context, it is essential to acquire a comprehensive understanding of the diverse range of techniques and technologies currently employed in indoor positioning. Furthermore, it is crucial to assess the merits, drawbacks, and key characteristics associated with each technique and technology in order to obtain a comprehension of indoor positioning. Generally, indoor positioning methods incorporate a variety of localization resources, including the received signal strength indicator (RSSI) [9, 10], angle of arrival (AOA) [11], channel state information (CSI) [12], fingerprinting/scene analysis, time of flight (ToF) [13], time difference of arrival (TDoA) [14], return time of flight (RToF) [15], and phase of arrival (PoA) [16]. Table 2 provides a brief overview of the advantages and disadvantages of these localization techniques [18, 19].

The first technique discussed is the RSSI-based method, which stands out due to its simplicity, affordability, and

Table 2
Comparison between different localization techniques [18, 19].

Technique	Advantages	Disadvantages
RSSI [9, 10]	Simple to do, affordable, and can be used with a number of technologies.	Prone to multipath fading and environmental noise, Fingerprinting may be necessary at lower localization accuracy.
CSI [11]	More resilient to indoor noise and multi-trajectories.	On commercially available NICs, it is not always accessible.
AoA [12]	Can provide high localization accuracy, does not require any fingerprinting.	Might require directional antennas and complex hardware, requires comparatively complex algorithms and performance deteriorates with increase in distance between the transmitter and receiver.
ToF [13]	Provides high localization accuracy, does not require any fingerprinting.	Require time stamps and multiple antennas at the transmitter and receiver to ensure that the transmitters and receivers are in synchronization with one another. Line of Sight is mandatory for accurate performance.
TDoA [14]	Does not need any fingerprinting, does not require clock synchronization among the device and RN.	Requires clock synchronization among the RNs, might require time stamps, requires larger bandwidth
RToF [15]	Does not require any fingerprinting, can provide high localization accuracy.	Requires clock synchronization, processing delay can have an impact on short-range measurement performance.
PoA [16]	Can be used in conjunction with RSS, ToA, TDoA to improve the overall localization accuracy.	reduced performance when the line of sight is not present.
Fingerprinting [17]	Reasonable ease of use.	Even when there is a slight change in the space, new fingerprints are necessary.

compatibility with diverse technologies. Nonetheless, its susceptibility to multipath fading and environmental noise poses a challenge to its accuracy. In certain scenarios, the utilisation of fingerprinting becomes necessary to achieve higher localization accuracy [20]. The second technique examined is the CSI-based method, which exhibits greater resilience to indoor noise and multi-trajectories compared to RSSI. However, the accessibility of CSI is not always guaranteed in commercially available network interface cards (NICs) [21]. Next, the AoA-based technique is explored, which offers a high level of localization accuracy without the need for fingerprinting. Nevertheless, the implementation of directional antennas and complex hardware may be required, and the involved algorithms tend to be relatively intricate. Additionally, the performance of AoA deteriorates as the distance between the transmitter and receiver increases [22]. The ToF-based technique is then discussed, which achieves high localization accuracy without reliance on fingerprinting. However, it necessitates the availability of time stamps and multiple antennas at both the transmitter and receiver to ensure synchronization. Furthermore, the accurate performance of ToF depends on the line-of-sight conditions.

The TDoA-based method is presented as another fingerprinting-free technique that does not require clock synchronization between devices and reference nodes (RNs) [18]. Nonetheless, time stamps and larger bandwidth may be necessary for its implementation. The RToF-based technique is introduced, which also eliminates the need for fingerprinting and offers high localization accuracy. However, clock synchronization is imperative, and the performance of short-range measurements may be affected by processing delay [23]. The PoA-based method can be employed in conjunction with RSSI, ToA, and TDoA techniques to enhance overall localization accuracy. However, its performance is diminished in the absence of line of sight. Lastly, fingerprinting is examined as a localization technique that offers reasonable ease of use. Nevertheless, any slight alterations in the physical space may require the creation of new fingerprints [19].

This study incorporates a range of techniques that utilise diverse technological approaches, encompassing radio communication technologies such as IEEE 802.11 (Wi-Fi) [24], UWB [25], radio frequency identification devices (RFID) [26], Bluetooth [27], ultrasound [22], and visible light [28]. Moreover, the utilisation of visible light and acoustic-based technologies [29] is also prominent. For a comprehensive comparison between these technologies, Table 3 presents a summary of the merits and drawbacks associated with these technologies, as reported in references [30]. This table presents a comparison of various localization technologies based on their maximum range, power consumption, advantages, and disadvantages. Wi-Fi is a widely available technology that offers high accuracy and does not require complex additional hardware. However, it is prone to noise and necessitates complex processing algorithms. UWB technology provides immunity to interference and delivers high accuracy. Nonetheless, it has a shorter range, requires extra hardware on different user devices, and comes with a higher cost. RFID has a wide range and low power consumption. However, its localization accuracy is relatively low. Bluetooth offers high throughput, reception range, and low energy consumption. Yet, it exhibits weak positioning accuracy and is susceptible to noise. Ultrasound technology covers a range of a few tens of meters and has comparatively less absorption. However, its effectiveness heavily relies on sensor placement. Visible Light technology can achieve a range of

Table 3
Comparison between localization technologies [30].

Technology	Maximum Range	Power Consumption	Advantages	Disadvantages
Wi-Fi [24]	250 m outdoor 35 m indoor	medium	Widely available, high accuracy, does not require complex extra hardware	Prone to noise, requires complex processing algorithms
UWB [25]	10-20 m	medium	Immune to interference, provides high accuracy	Shorter range, requires extra hardware on different user devices, and high cost
RFID [26]	200 m	Low	Has a wide range and uses little power	Low localization accuracy
Bluetooth [27]	100 m	Low	High throughput, reception range, low energy consumption	Weak positioning accuracy and susceptible to noise
Ultrasound [22]	Couple-tens of meters	Low-Moderate	Comparatively less absorption	High dependence on sensor placement
Visible Light [28]	1.4 km	Relatively higher	High dependence on the sensor placement	Obstacles reduce range and mostly require LoS
Acoustics [29]	Couple of meters	Low-Moderate	Can be used for proprietary applications can provide high accuracy	Affected by sound pollution and requires extra anchor points or hardware

up to 1.4 km but is relatively higher in power consumption. It also depends significantly on sensor placement and its effectiveness is reduced by obstacles, often requiring line-of-sight conditions. Acoustics technology operates within a range of a few meters and can provide high accuracy for proprietary applications. However, it is affected by sound pollution and necessitates extra anchor points or hardware. These localization technologies offer a range of capabilities and trade-offs, making them suitable for different use cases depending on the specific requirements and constraints of the application [31, 32, 33].

3. Preliminaries

This section introduces the formulation techniques (Subsections 3.1 and 3.2) and outlines the performance evaluation method (Subsection 3.3) for the proposed system.

3.1. Spatial fingerprinting technique

The Wi-Fi technology explored in this work are widely employed and straightforward method for indoor positioning [34]. In this study, the PDR approach is employed in conjunction with the inertial sensors of the smartphone, including the accelerometer, gyroscope, and magnetometer. This allows for the collection of real-time data while the user is walking. The collected magnetic readings are compared with the magnetic fingerprint of an offline map. The output of the PDR approach serves as the motion model in the fusion process to determine the user's position, while the magnetic data is utilised in the monitoring model [26, 23].

The fingerprint based on the indoor localization system includes two main stages:

1. *Offline stage*: In this stage, the RSS samples are gathered at predefined locations known as reference points (RPs).
2. *Online stage*: In this stage, the users' positions are established by comparing real-time RSS estimates to the database, as shown in Fig. 1.

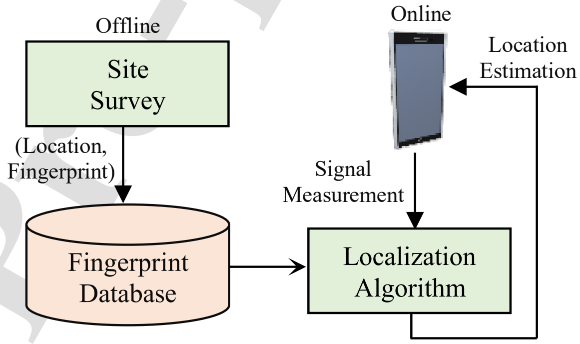

Figure 1: An overview of fundamental system flow for indoor localization through fingerprinting.

Due to the dependence of the indoor localization strategy on the magnetic fingerprint, which is utilised to calibrate the results of the PDR approach, Wi-Fi fingerprinting is typically conducted in two phases:

1. *The offline phase (survey)*: In this phase, the vector of RSS_i of all detected Wi-Fi signals from N number of access points AP_i, $\forall i = \{1, \cdots, N\}$, at multiple reference points of recognized positions are collected during a site assessment. Hence, the fingerprint of each RP is used to represent it [35, 36]. The fingerprints of the site are formed by aggregating all the RSS vectors, which are then stored in a database for subsequent online queries.
2. *The online phase (query)*: When the user (or object) samples or measures an RSS vector, the server compares it with the stored fingerprints using a similarity metric in the signal space, such as the Euclidean distance. This allows the server to identify the "neighbouring" fingerprints that are most similar to the received RSS vector [37]. The target position is then calculated based on these neighbouring fingerprints,

taking into consideration their similarities to the measured RSS vector.

Finally, pure Wi-Fi-based indoor positioning may introduce considerable errors, which can be mitigated by incorporating IMU data and employing position estimation techniques such as particle filtering. To achieve highly accurate indoor localization using RSS estimates, certain principles and guidelines need to be followed. For instance, the reference points should be easily identifiable with at least one access point and strategically positioned throughout the area of interest to ensure accurate and reliable data collection during user movement. Additionally, generating an offline magnetic field fingerprint map and performing online positioning involve comparing the observed magnetic field with the fingerprints stored in the database [38]. These measures contribute to enhancing the precision and correctness of Wi-Fi-based indoor localization systems. The proposed method focuses on the generation of an RSSI chart for the specified test area, serving as a viable alternative to the extraction of personalized fingerprints for each user.

3.2. PDR-based site surveying technique

The PDR technique is a highly effective approach for indoor positioning, involving three main stages: (I) step detection, (II) step length estimation, and (III) walking direction determination, as depicted in Fig. 2. Fig. 2(a) illustrates the 2D coordinates associated with each step undertaken during the process of data collection, whereas Fig. 2(b) depicts the distinction between the path-based and point-based methodologies employed in data collection. In the path-based approach, data is collected systematically along predefined paths or trajectories within the environment. These paths can be specific routes or walkways. On the other hand, the point-based approach involves the collection of data at discrete, strategically selected locations within the environment, with the selection of these points often guided by the attributes or parameters being measured. The proposed algorithm employs the path-based methodology for site surveying, primarily chosen for its exceptional accuracy and reliability. The PDR technique offers advantages such as simplifying the path loss model and improving reliability, particularly in large areas. Unlike fingerprinting, which requires a lengthy training process, the PDR approach leverages measurements from integrated IMU sensors in a smartphone, including magnetometers, accelerometers, gyroscopes, and barometers. These sensors enable the measurement of direction, acceleration, rotational velocity, and altitude. If the initial location is known, the device can be tracked using dead reckoning.

The accelerometer is utilised for step counting and estimating step length, while the accelerometer, magnetometer, and gyroscope are utilised to measure the differences between two consecutive steps [39, 40]. It is important to highlight that magnetic field data, despite its inherent noise when employed for localization, presents significant advantages for positioning due to its capacity to detect even minor alterations in the three-dimensional behaviour of the magnetic field, as discerned by the magnetometer within the IMU sensors. Notably, this magnetic field data demonstrates a remarkable level of measurement stability that persists over time, thereby establishing it as a viable and apt choice for facilitating assisted localization endeavours.

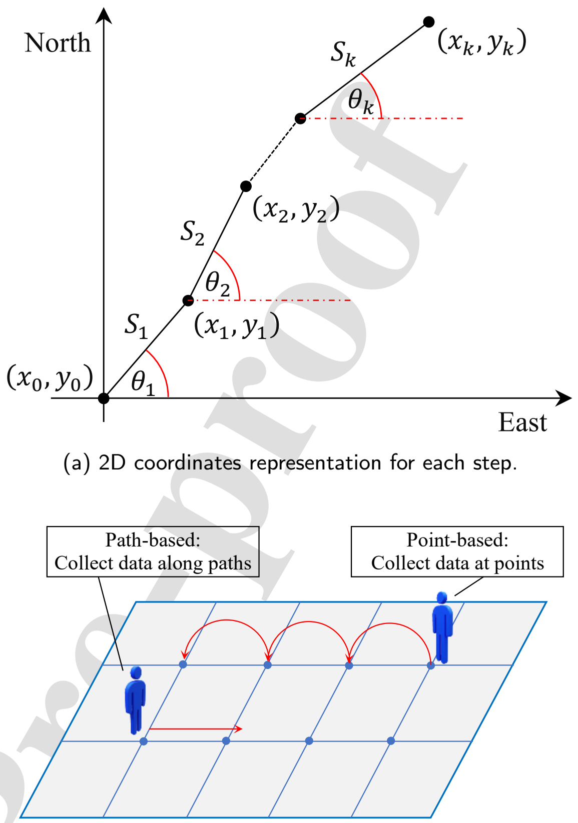

(a) 2D coordinates representation for each step.

(b) The two types for the data collection approach.

Figure 2: Location estimation and data gathering with UWB and IMU by PDR approach.

3.3. RSSI-based method

UWB devices can be employed for user equipment positioning through the utilisation of the trilateration method. UWB technology offers the advantage of high-precision distance measurements by utilising short-duration, wideband radio pulses. When multiple UWB anchors with known positions are strategically placed, they can enable accurate trilateration, leading to precise UE positioning based on the measurement of the time it takes for UWB signals to travel between the device and the anchors, see Fig. 3. As the RSS value increases, the distance between Tx and Rx decreases. A minimum of three UWBs (UWB_i, $\forall i = \{1, \cdots, M\}$) are needed to determine the position of the UE, where M represents the number of the UWB anchors [32]. The positioning error decreases as the number of M increases, and conversely, it increases as the number of M decreases.

This method employs the radio propagation model to calculate the distance, which can be characterised as follows:

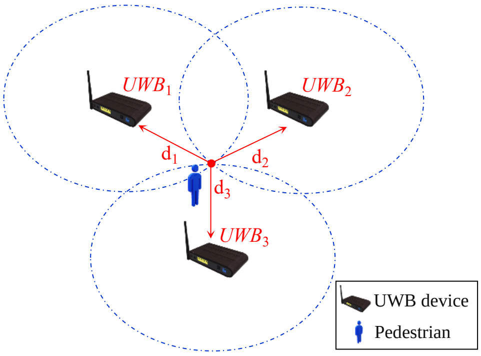

Figure 3: Position computation utilising trilateration method based on RSS measurements.

$$P_t^i = P_0 - \left(10\,\eta \log_{10} \frac{d_t^i}{d_0}\right) \tag{1}$$

where P_t^i demonstrates the RSS from the UWB_i and d_t^i signify the space from the UWB_i during the step t. The parameter P_0 is the RSS at a reference distance d_0, which is typically one meter [33]. Typically, P_0 is considered equivalent to the power transmitted from the UWB device. The trajectory loss exponent is represented by η and its value is considered to range from 1.5 to 7.2 for a complex indoor environment. So, by utilising (1), the distance d_t^i can be defined as:

$$d_t^i = 10^{\left(\frac{P_0 - P_t^i}{10\,\eta}\right)} \tag{2}$$

In the Cartesian coordinates, it can be expressed as

$$d_t^i = \sqrt{(X - x_i)^2 - (Y - y_i)^2} \tag{3}$$

where (x_i, y_i) represents the two-dimensional (2D) coordinates of the UWB_i and (X, Y) is that of the pedestrian. The estimated RSS (RSS_i) of the signal received from UWB_i is then converted into the corresponding distance between the UE and UWB_i using (2).

4. System and scheme modelling

This section introduces the system model and provides a comprehensive discussion of the proposed scheme.

4.1. Overview

For a clear understanding of the proposed approach, it consists of two stages: collecting reference fingerprints and performing location estimation.

4.1.1. Stage 1: Collection of reference fingerprints

Reference fingerprints constitute a dataset of Wi-Fi signal characteristics gathered from different locations within the test area, serving as reference points for subsequent localization. This collection process encompasses the following steps:

1. *Placement of access points*: Strategically positioning Wi-Fi access points across the test area to ensure sufficient coverage.
2. *Signal measurement*: Employing devices equipped with Wi-Fi receivers, such as smartphones, to measure the RSS from nearby AP at predefined locations.
3. *Data recording*: Recording the measured signal characteristics alongside the corresponding location details to establish the reference fingerprint dataset.

4.1.2. Stage 2: Location estimation

Upon the collection of reference fingerprints, the process of localizing a target device goes through the following typical steps:

1. *Signal sampling*: The target device, often a smartphone, continually scans and samples the Wi-Fi signals in its vicinity.
2. *Signal matching*: The sampled Wi-Fi signal characteristics are compared to the reference fingerprints stored within the dataset, with the objective of identifying the closest match based on signal similarity.
3. *Location estimation*: Upon discovering a match, the associated location information linked to the reference fingerprint is designated as the estimated location of the target device.

4.2. System modelling

The system comprises two primary components, Wi-Fi devices and smartphone inertial sensors integrated within the UE. For testing, ultra-wideband devices are employed to calculate the reference or actual trajectory of the UE within the designated test area. Each device has a specific role defined as follows.

1. *Wi-Fi devices*: These devices, as part of the system, play a significant role in facilitating wireless connectivity and data exchange. They utilise Wi-Fi technology to establish communication within the system and contribute to the localization process. These devices provide additional information such as signal strength and connectivity patterns, which are utilised for positioning and tracking purposes in conjunction with other devices.
2. *Smartphone inertial sensors*: Smartphones are equipped with various sensors, such as the accelerometer, magnetometer, and gyroscope, that can measure different physical quantities related to the smartphone's movement and orientation. The measurements of these sensors are used as input to the PDR technique to estimate the user's position and track their movement.
3. *Pozyx ultra-wideband devices*: In the system, the UWB devices, also referred to as anchors and rover devices operate in conjunction with a network of devices placed at fixed and predetermined locations. The tag, connected to the smartphone's inertial sensors, captures UWB measurements and timestamps throughout the designated experimental area. Trilateration is employed to calculate the distances between

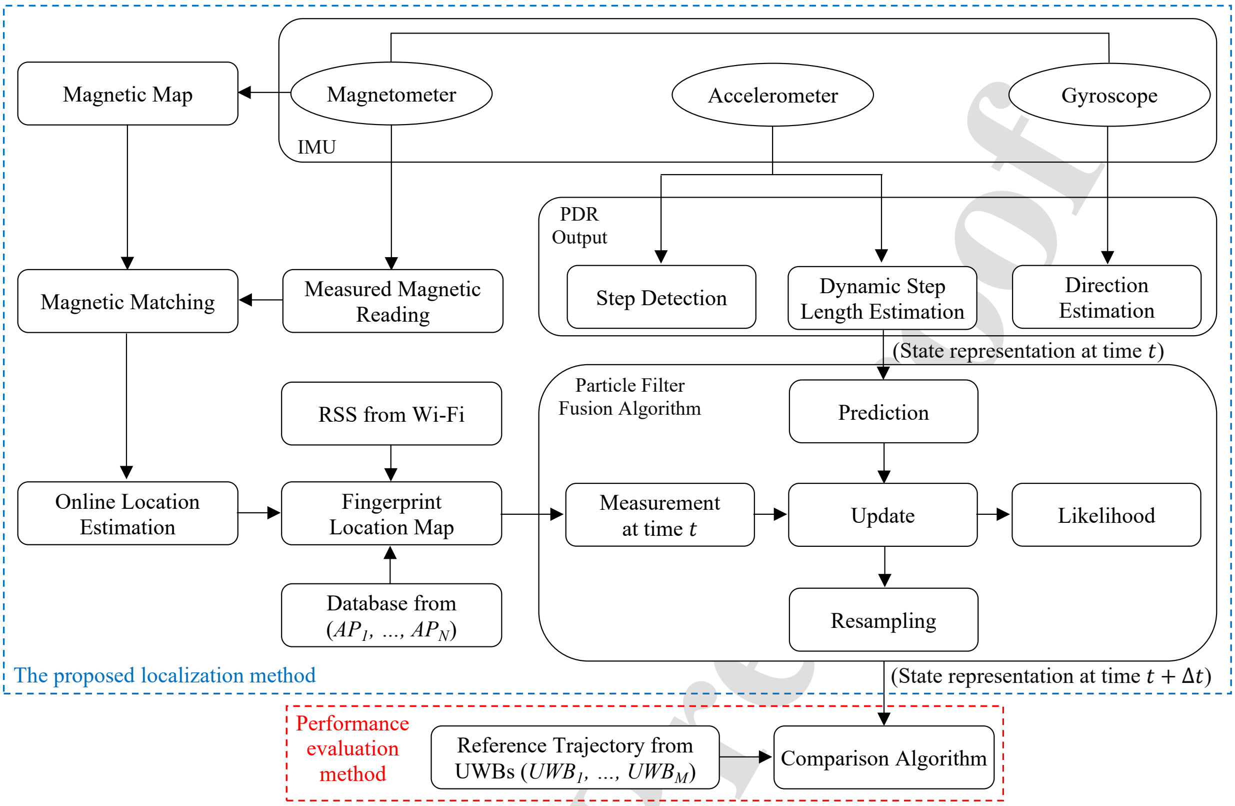

Figure 4: The proposed method architecture and the evaluation method.

the UE and anchors, yielding a near-actual trajectory for assessing the proposed method's accuracy. It is important to note that precise calibration of UWB readings is essential to accurately model the range error and achieve improved localization accuracy.

4.3. Scheme modelling

This research paper presents a novel system, depicted in Fig. 4, that introduces an enhanced indoor positioning solution characterised by improved reliability, cost-efficiency, and accuracy. The proposed system leverages the particle filter algorithm and integrates data obtained from various sensors or crowd-sensing techniques. The data collection process occurs within the designated test area, as previously mentioned. The system involves the meticulous scanning of the test area by the user. The IMU features embedded in the user's smartphone are utilised to enable positioning using the PDR method. Additionally, measurements of the magnetic field obtained from Wi-Fi RSS are captured to construct a magnetic map employing fingerprinting techniques. Consequently, a magnetic database specific to the test region is developed. The collected data from the aforementioned sources are synchronized, fused, and subsequently transmitted to the particle filter algorithm. In this context, we discuss in detail the particle filter fusion algorithm and the positioning method used in the proposed scheme.

4.3.1. Particle filter fusion algorithm

Fig. 5 depicts the flowchart of the proposed system, which highlights the process of matching various data derived from crowdsensing through the PDR approach. These data are subsequently fed into the particle filter algorithm to predict the new location and generate a path. The generated path is then compared with the reference trajectory obtained from UWB anchors. Furthermore, the system leverages Wi-Fi devices positioned at strategic locations within the test area to construct a magnetic map. This map is pre-drawn and computed to capture acceleration data using a set of N access points. The magnetic map serves as a fingerprinting database, enabling synchronization to identify the access point with the highest RSS within the test area. This data is then utilised to update the particle filter and enhance the accuracy of localization. By comparing the particle filter's trajectory with the reference path, the closest match is determined for evaluation. Additionally, the mutual information method is employed to facilitate a comprehensive comparison and assessment of the results.

4.3.2. The positioning algorithm

The particle filter (PF) plays a crucial role in the proposed system as it serves as a probabilistic estimator capable of handling non-Gaussian and nonlinear processes. This estimation technique relies on random samples, known as particles, to recursively approximate the target distribution.

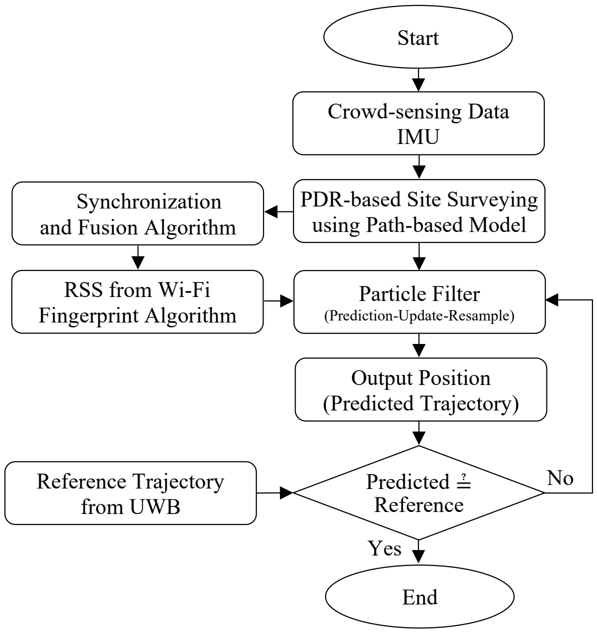

Figure 5: The flowchart of the proposed system and the evaluation process.

The PF offers several advantages, including the ability to estimate full probability density functions (PDFs), efficiency in concentrating particles in high probability regions, and the capability to handle non-linear state and observation models. In order to gain a deeper understanding of the PF's operation within the proposed system, it is important to discuss its key steps, see Fig. 4.

1. *State representation or initialisation step*: The pdf of the state values is described using (n-particles) instead of a second-order statistical description. As a result, the PDF $p(x)$ can be expressed as

$$p(x) = \int_{i=1}^{n} w_i K\left(x - x_i\right) \tag{4}$$

where w_i is the weight of the i^{th} particle, and $K(x)$ is the basis function. If we assume that $K(x)$ is Dirac's delta function, the particle representation of $p(x)$ with equal weights can be exemplified as

$$p(x) = \frac{1}{n}\int_{i=1}^{n} \delta\left(x - x_i\right) \tag{5}$$

2. *Prediction step*: Update the particle's state by applying the state transition function for each particle i as follows.

$$p\left(x_{t+\Delta t}/y_{0,\dots}y_t\right) = \int p\left(x_{t+\Delta t}/x_t\right) p\left(x_t/y_{0,\dots}y_t\right) dx_t \tag{6}$$

$$p\left(x_{t+\Delta t}/y_{0,\dots}y_t\right) = \sum_{i=1}^{n} w_{t,i}\, p\left(x_{t+\Delta t}/\bar{x}_{t,i}\right) \tag{7}$$

where $w_{t,i}$ is the weight factor. After sampling $\hat{x}_{t,i}$ the equation of prediction can be expressed as

$$p\left(x_{t+\Delta t}/y_{0,\dots}y_t\right) = \sum_{i=1}^{n} \frac{1}{n}\delta\left(x_t - \hat{x}_{t,i}\right) \tag{8}$$

3. *Update step*: In this step, the algorithm evaluates the likelihood or probability of the RSS measurements given the predicted state of the system. Then, we undertake the computation of likelihood values, while taking into account the inherent noise and uncertainties, to establish a quantitative assessment of the degree of concordance between estimated and actual measurements. To refine the accuracy of our particle filter fusion algorithm, we then proceed to update the weights of the individual particles based on their respective likelihood values, assigning higher weights to those particles that exhibit measurements in closer proximity to the actual sensor measurements. In situations where the probability is primarily concentrated on a limited set of state values, the weights associated with these values can diminish significantly, leading to extremely low probabilities. To mitigate this challenge, we employ a resampling procedure aimed at substituting a particle with a substantial weight, which has a higher likelihood of being selected multiple times, while a particle with a low weight is unlikely to be chosen at all. The resultant equations governing the update step can be expressed as

$$p\left(x_t/y_{0,\dots}y_t\right) = \int_{i=1}^{n} \frac{1}{n}\delta\left(x_t - \bar{x}_{t,i}\right) \tag{9}$$

$$p\left(x_{t+\Delta t}/y_{0,\dots}y_{t+\Delta t}\right) = \int_{i=1}^{n} \frac{1}{n}\delta\left(x_{t+\Delta t} - \bar{x}_{t+\Delta t,i}\right) \tag{10}$$

4. *Particle resample step*: The degeneracy problem, which occurs when only a few particles have a high weight while the rest have very low weights, can be solved by using the resampling step. This problem can be identified using an effective sample size estimate from the following equation:

$$N_{eff} = \frac{1}{\int_{i=1}^{n}\left(w_{t,i}\right)^2} \tag{11}$$

4.3.3. RSS-based reference trajectory estimation algorithm

This algorithm employs the received data to predict the user's current position and generates a reference trajectory that closely aligns with the UE's actual path for further comparative analysis. UWB devices are strategically deployed within the test area to establish a reference trajectory through the implementation of the trilateration method. Subsequently, this reference path serves as a basis for comparison with the anticipated trajectory generated by employing the particle filter algorithm in conjunction with the mutual information method. The dynamic model for computing the reference trajectory can be presented as:

$$\begin{bmatrix} \hat{x}(t+\Delta t) \\ \hat{y}(t+\Delta t) \end{bmatrix} \approx \begin{bmatrix} \hat{x}(t) \\ \hat{y}(t) \end{bmatrix} + \Delta t \begin{bmatrix} \hat{v}_x(t) \\ \hat{v}_y(t) \end{bmatrix} \tag{12}$$

$$\begin{bmatrix} \hat{v}_x(t+\Delta t) \\ \hat{v}_y(t+\Delta t) \end{bmatrix} = \begin{bmatrix} \hat{v}_x(t) \\ \hat{v}_y(t) \end{bmatrix} + \begin{bmatrix} \hat{e}_{v,x}(t) \\ \hat{e}_{v,y}(t) \end{bmatrix} \tag{13}$$

where $[\hat{x}(t), \hat{y}(t)]^T$ and $[\hat{x}(t+\Delta t), \hat{y}(t+\Delta t)]^T$ are the 2D positions at times t and $t+\Delta t$, respectively, $[\hat{v}_x(t), \hat{v}_y(t)]^T$ are the two dimension velocity at time t, $[\hat{e}_x(t), \hat{e}_y(t)]^T$ are the difference variable at time t, and Δt is the time interval between two sequential UWB transceiver devices.

The optimisation equation for obtaining the reference trajectory of UWB devices in the trilateration problem, assuming a fixed altitude of the device in the $\overline{z}$ direction, can be expressed as

$$[\hat{x}(i)\ \ \hat{y}(i)] = \arg\min_{x_i, y_i} \sum_i \sum_j \frac{\left(\hat{d}_j(i) - r_j(i)^2\right)^2}{\sigma_r^2} \tag{14}$$

$$\hat{d}_j(i) = \sqrt{\left(x_i - x_{anch,j}\right)^2 + \left(y_i - y_{anch,j}\right)^2} \tag{15}$$

where $[\hat{x}(i)\ \ \hat{y}(i)]$ represents the calculated coordinates corresponding to the UWB_i time sample, $r_j(i)$ denotes the measurement obtained from the j^{th} anchor at the UWB_i time sample, σ_r represents the uncertainty associated with UWB measurements (assuming a zero-mean Gaussian distribution for simplicity), and $[x_{anch,j}\ \ y_{anch,j}]$ denote the location of the j^{th} anchor.

5. Experimental Results and Discussion

This section presents the experimental findings of the proposed scheme. Firstly, the experiment is conducted in a pair of corridors on the second level of a building at the University of Padua in Italy. One corridor measures approximately 40 meters in length, while the other corridor is approximately 12 meters long. The experiment area is equipped with 11 Pozyx ultra-wideband devices and eighteen Wi-Fi devices (i.e., $N = 18$ access points) positioned on the tops of the two corridors. The map of the corridors is illustrated in Fig. 6.

In this experiment, the Pozyx UWB devices are positioned within the test area to establish a reference trajectory through the utilisation of the trilateration method. This

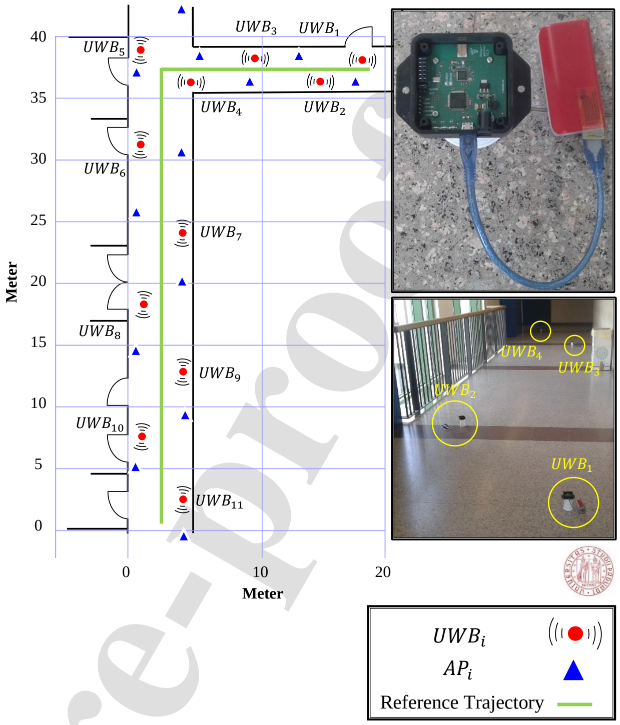

Figure 6: The map of the test area and the reference trajectory using UWBs.

reference path serves as a basis for comparison with the predicted trajectory generated using the particle filter and mutual information method. In this experiment, a total of 11 UWBs are employed. Subsequently, the user proceeds to carefully traverse back and forth in the corridor adjacent to the CIRGEO lab. This movement generates three distinct tracks: one in the centre of the hallway, another adjacent to the wall, and a third in close proximity to the windows. The sampling rate of the IMU in LG Android smartphones can range from 100 Hz to 200 Hz. The IMU features integrated within the smartphone are leveraged to momentarily pause at the conclusion of each run before recommencing, allowing for the collection of data using the PDR method. Measurements of the magnetic field from Wi-Fi RSS are also obtained, enabling the creation of a magnetic map using fingerprinting techniques. Subsequently, a magnetic database is constructed specifically tailored to the test region.

The acquired data, encompassing the UWB, IMU, and magnetic field measurements, are then synchronized, fused, and conveyed to the particle filter. This filtering mechanism facilitates the prediction of the new position and draws a trajectory that closely aligns with the reference path, enabling subsequent comparison and evaluation. Table 4 lists the localization algorithm implemented in the proposed system, outlining the complete sequence of operations involving the particle filter and crowd-sensing on the designated test area.

Fig. 6 illustrates the reference trajectory computed using the trilateration method with UWB anchors ($UWB_i, \forall i = \{1, \cdots, 11\}$). The green solid line represents the reference

Table 4
Positioning Algorithm based on the particle filter.

Step 1: Utilising Pozyx UWB anchors and IMU to collect data by PDR method.
Step 2: Utilising Matlab to preprocess data and then load the processed data.
Step 3: Representing the phase one (3 tracks) and the 2D trajectory predicted by UWB.
Step 4: Displaying points of the initial to the third path in stage one (which is split into 6 sub-paths).
Step 5: Defining Wi-Fi measurements and displaying the RSS vs. time relationship.
Step 6: Measuring Magnetic Fields directions.
Step 7: Creating the fingerprinting database for the test of area.
Step 8: Particle filter process.
Step 8.1: State representation or initialisation using (5)
Step 8.2: Applying the Prediction step using (8)
Step 8.3: Applying the Update step: using (10)
Step 8.4: Applying the Particle Resample step using (11)
Step 9: Particle filter loop to compute the predicted location and drawing trajectory.
Step 10: Utilising the mutual information and reference trajectory for matching and comparing with the particle filter's predicted trajectory.

trajectory for the trial region, while the red circles signify the 11 UWB devices, each accompanied by a number (UWB_i) indicating the UWB anchor.

5.1. The obtained UWB trajectories

Fig. 7 presents a comprehensive overview of the data collected during the experiment, showcasing the three distinct tracks: left, central, and right. These tracks serve as the training dataset for the fingerprinting process utilising IMUs with path-based movement within the test region. Additionally, the figure depicts the resultant 2D trajectory computed via UWB technology. In order to increase the learning dataset of the test region and use it as a database for fingerprinting, the PDR approach is employed to collect data at the centre of the test area, both in forward and backward directions, thereby creating the central track. This process has been repeated six times, resulting in six sub-tracks, see Fig. 7(b). The same process was repeated on the left side, creating six additional sub-tracks, see Fig. 7(c). Similarly, data is collected on the right side, resulting in four sub-tracks, see Fig. 7(d). Note that, we generated many sub-tracks for each main track. However, we choose the best-estimated sub-tracks that present the left, central, and right sides of the corridor. Finally, Fig. 7(a) illustrates all computed reference trajectories using the trilateration method and the estimated UWB anchors.

5.2. The particle filter process

The inclusion of the particle filter in the proposed method enhances the accuracy and effectiveness of predicting the position and trajectory within the trial region. This improvement is achieved by leveraging data obtained through the PDR approach and IMU, along with continual updates from the magnetic fingerprint database. Subsequently, the computed trajectory is compared to the reference trajectory with a high probability of matching. This process involves utilising particles and connecting them to the synchronized 18 access points. These access points are synchronized with the central server. Fig. 8 and 9 provide visual representations of the RSS estimates, the distribution of particles, and the resampling step of the particle filter, specifically for the best 13 out of the 18 access points. In the first column of Fig. 8 and Fig. 9, the RSS values (RSS_i) from AP_i are presented for $i = \{1, \cdots, 7\}$ and $i = \{8, \cdots, 13\}$, respectively. The second column of Fig. 8 and Fig. 9 illustrate the distribution of n particles at a certain time-slot for AP_i, where $i = \{1, \cdots, 7\}$ and $i = \{8, \cdots, 13\}$, respectively. The distribution is presented within the tested area's map defined in Fig. 6. Finally, the third column of Fig. 8 and Fig. 9 depict the resampling process of the particles for AP_i, with $i = \{1, \cdots, 7\}$ and $i = \{8, \cdots, 13\}$, respectively.

The resampling process effectively addresses the degeneracy problem, wherein only a few particles possess significant weights while the majority of particles have exceedingly small weights. During resampling, particles with substantial weights are selected multiple times, while those with low weights are unlikely to be chosen. In the context of our experiment, the resampling process exhibits two distinct behaviours contingent upon the particle's weight, as presented in the third column of Fig. 8 and Fig. 9. Specifically, when the weight exceeds or equals the threshold of -70, the particle is deemed eligible for consideration in our experimental analysis. Conversely, particles failing to meet this weight criterion are excluded from further consideration.

Following the completion of all the operations and steps described earlier, the particle filter can predict and estimate the magnetic path by fusing all the data obtained from crowd-sensing, as illustrated in Fig. 10. Table 5 summarises the performance metrics of different methods. These methods are evaluated in terms of enhanced accuracy and average error. The first method corresponds to the IMU and PDR approach without a magnetic fingerprinting database, achieving an enhanced accuracy of 80.49% with an average error of 0.3. In contrast, the second method presents results for the IMU and PDR approach when incorporating a magnetic fingerprinting database, showing an enhanced accuracy of 85.86% and an average error of 0.32. Finally, the proposed method employs a particle filter with 1000 particles and a magnetic fingerprinting database. This method demonstrates a significantly improved enhanced accuracy of

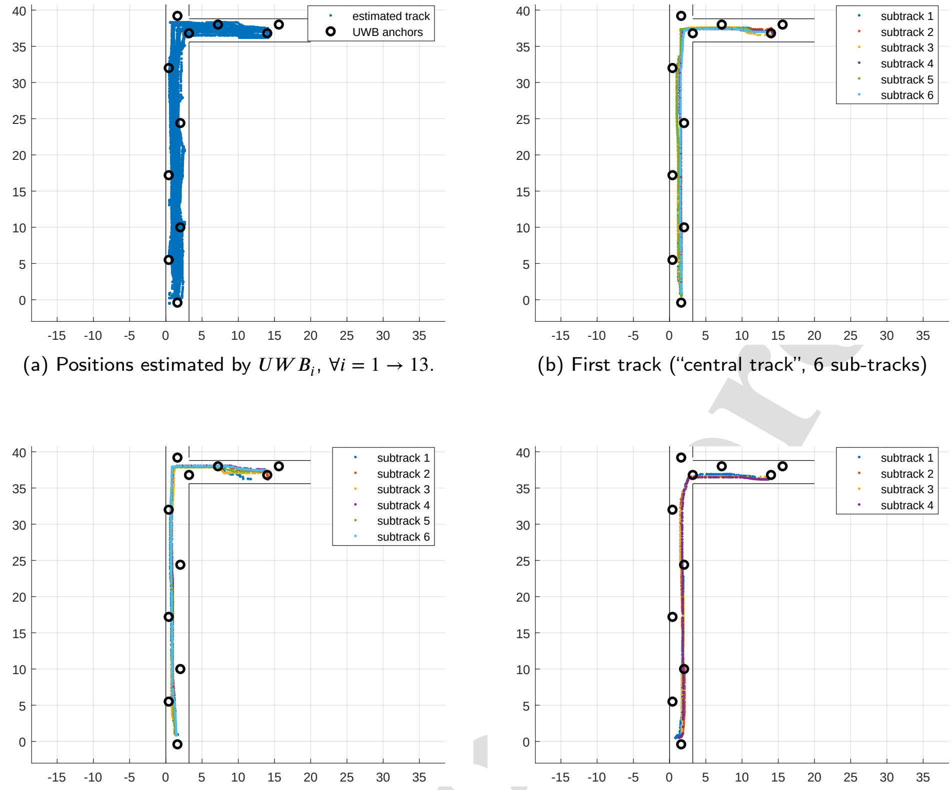

(a) Positions estimated by UWB_i, $\forall i = 1 \rightarrow 13$.

(b) First track (“central track”, 6 sub-tracks)

(c) Second track (“left track”, 6 sub-tracks)

(d) Third track (“right track”, 4 sub-tracks)

Figure 7: Computed paths using UWB_i devices, $\forall i = 1 \rightarrow 11$, and tracks using the IMU.

Table 5
Comparison between the root mean square error (RMSE) values for the trajectory states obtained using the IMU, PDR, and particle filter and magnetic fingerprinting with reference trajectory using UWB.

Algorithm	Enhanced accuracy	Average error to the reference trajectory
IMU and PDR approach without magnetic fingerprinting database	80.49%	0.3
IMU and PDR approach with magnetic fingerprinting database	85.86%	0.32
The proposed method using the particle filter of $n = 1000$ particles and magnetic fingerprinting database	96.32%	0.359

96.32% while maintaining an average error of 0.359. Based on these findings, we conclude that the proposed method achieves the highest level of accuracy, which attains an enhanced accuracy of 96.32%. However, this approach does exhibit the largest average error in the last column from Table 5, indicating an average error of 0.359. Therefore, while the proposed method significantly improves accuracy, it does come at the expense of a slightly higher average error. The choice of which approach is “best” depends on the specific trade-off between accuracy and average error that aligns with the application’s objectives and requirements.

6. Conclusions

This paper provides an overview of indoor positioning technologies, methodologies, strategies, and contemporary applications. Additionally, the paper presents a low-cost, reliable, and highly accurate indoor localization system based on crowdsensing, particle filter, and the test region’s infrastructure. Furthermore, the system relies on the RSS signals from Wi-Fi devices equipped in the test area, and the signals from access points are synchronized to build a magnetic fingerprinting database used for acceleration. This approach overcomes the limitations of traditional magnetic

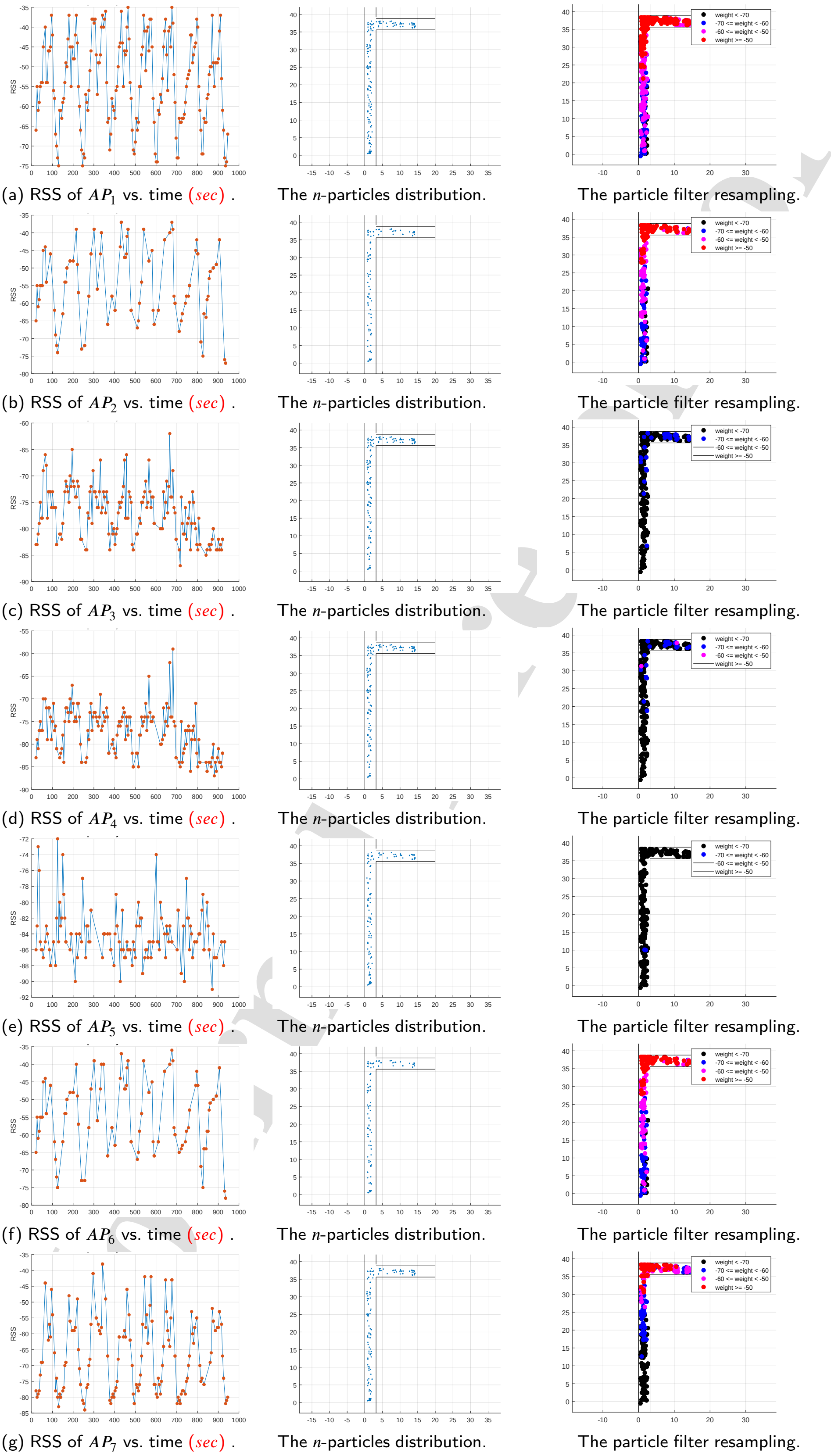

(a) RSS of AP_1 vs. time (sec) . The n-particles distribution. The particle filter resampling.

(b) RSS of AP_2 vs. time (sec) . The n-particles distribution. The particle filter resampling.

(c) RSS of AP_3 vs. time (sec) . The n-particles distribution. The particle filter resampling.

(d) RSS of AP_4 vs. time (sec) . The n-particles distribution. The particle filter resampling.

(e) RSS of AP_5 vs. time (sec) . The n-particles distribution. The particle filter resampling.

(f) RSS of AP_6 vs. time (sec) . The n-particles distribution. The particle filter resampling.

(g) RSS of AP_7 vs. time (sec) . The n-particles distribution. The particle filter resampling.

Figure 8: The particle filter process linked with the synchronized access points for each AP_i, $\forall i = 1 \rightarrow 7$.

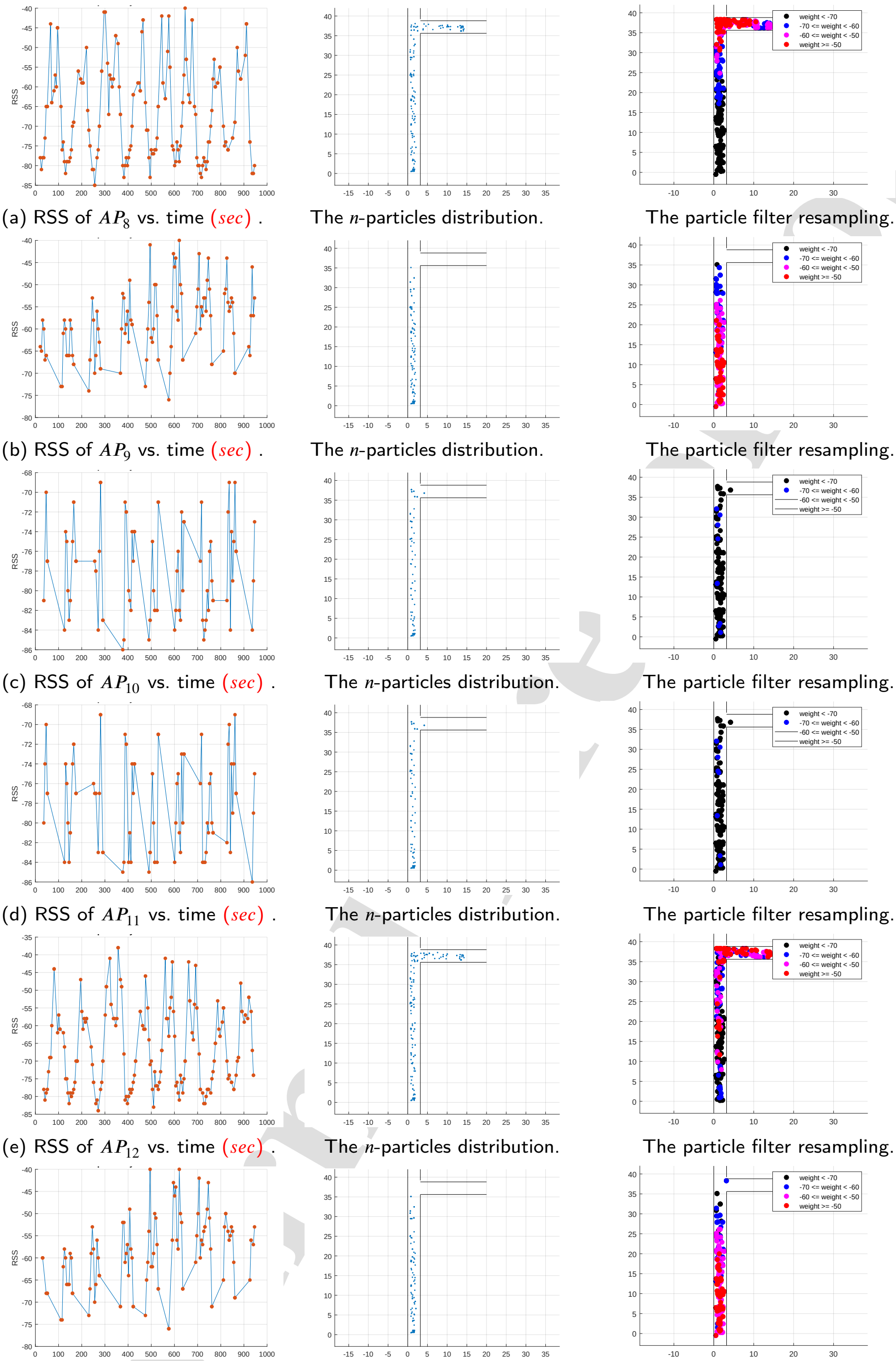

(a) RSS of AP_8 vs. time (sec) . The n-particles distribution. The particle filter resampling.

(b) RSS of AP_9 vs. time (sec) . The n-particles distribution. The particle filter resampling.

(c) RSS of AP_{10} vs. time (sec) . The n-particles distribution. The particle filter resampling.

(d) RSS of AP_{11} vs. time (sec) . The n-particles distribution. The particle filter resampling.

(e) RSS of AP_{12} vs. time (sec) . The n-particles distribution. The particle filter resampling.

(f) RSS of AP_{13} vs. time (sec) . The n-particles distribution. The particle filter resampling.

Figure 9: The particle filter process linked with the synchronized access points for each AP_i, $\forall i = 8 \rightarrow 13$.

Figure 10: The predicted trajectory using particle filter.

field-based localization techniques, which are heavy in terms of comparison workload and insufficient in analysing magnetic field signals that do not change easily over time. The system also employs continuous updating of the particle filter with data collected by the IMU, using the PDR method to obtain motion data such as acceleration, stride size, and direction to estimate the predicted trajectory. Finally, the proposed system's accuracy is demonstrated by comparing the estimated trajectory using the particle filter with the reference path using the UWB anchors through trilateration and the mutual information approach, which showed an improvement in accuracy from 80.49% to 96.32% using crowd-sensing, particle filter, and magnetic fingerprinting.

References

[1] Tiwari, S., and Jain, V.K. HILS: Hybrid indoor localisation system using Wi-Fi received signal strength and inertial sensor's measurements of smart-phone. *IET Communications*, 13 (11), (2019), 1595 – 1606.

[2] Gupta, A., and Fernando, X. Simultaneous localization and mapping (SLAM) and data fusion in unmanned aerial vehicles: Recent Advances and Challenges. *Drones*, 6(4), (2022).

[3] Gu, F., Hu, X., Ramezani, M., Acharya, D., Khoshelham, K., Valaee, S., and Shang, J. Indoor localization improved by spatial context—A survey. *ACM Comput. Surv.*, 52 (3), (2019), 1–35.

[4] Yang, T., Cabani, A., and Chafouk, H. A survey of recent indoor localization scenarios and methodologies. *Sensors*, 21 (23) (2021).

[5] Ashraf, I., Hur, S., Park, S., and Park, Y. DeepLocate: Smartphone based indoor localization with a deep neural network ensemble classifier. *Sensors*, (20 (1), (2020).

[6] Ciabattoni, L., Foresi, G., Monteriù, A., Pepa, L., Pagnotta, D.P., Spalazzi, L., and Verdini, F. Real time indoor localization integrating a model based pedestrian dead reckoning on smartphone and BLE beacons. *J. Ambient. Intell. Humaniz. Comput.*, 10, (2019), 1-12.

[7] Zhao, H., Cheng, W., Yang, N., Qiu, S., Wang, Z., and Wang, J.S. Smartphone-based 3D indoor pedestrian positioning through multi-modal data fusion. *Sensors*, 19 (20) (2019).

[8] Yao, Y., Pan, L., Feng, W., Xu, X., Liang, X., and Xu, X. A robust step detection and stride length estimation for pedestrian dead reckoning using a smartphone. *IEEE Sens. J.*, 20 (17), (2020), 9685-9697.

[9] Chandra, G. Position estimation at indoors using Wi-Fi and magnetic field sensors. In Proceedings of the IPIN 2022 WiP Proceedings, Beijing, China, (2022).

[10] J. Kaur et al., AI-enabled CSI fingerprinting for indoor localisation towards context-aware networking in 6G. 2023 IEEE Wireless Communications and Networking Conference (WCNC), Glasgow, United Kingdom, (2023).

[11] Khan, D., Cheng, Z., Uchiyama, H., Ali, S., Asshad, M., and Kiyokawa, K. Recent advances in vision-based indoor navigation: A systematic literature review. *Computers & Graphics*, (2022).

[12] Ta, V.-C., Dao, T.-K., Vaufreydaz, D., and Castelli, E. Collaborative smartphone-based user positioning in a multiple-user context using wireless technologies. *Sensors*, (2020

[13] Lashkari, B., Rezazadeh, J., Farahbakhsh, R., and Sandrasegaran, K. Crowdsourcing and sensing for indoor localization in IoT: A review. *IEEE Sensors Journal*, 19(7), (2019), 2408-2434.

[14] Yu, Y., Chen, R., Chen, L., Li, W., Wu, Y., and Zhou, H. Autonomous 3D indoor localization based on crowdsourced Wi-Fi fingerprinting and MEMS sensors. *IEEE Sensors Journal*, 22, (2021), 5248-5259.

[15] Xue, W., Hua, X., Li, Q., Yu, K., and Qiu, W. Improved neighboring reference points selection method for Wi-Fi based indoor localization. IEEE Sensors Letters, 2(2), (2018), 1-4.

[16] Gasparetto, A., Boscariol, P., Lanzutti, A., and Vidoni, R. Path planning and trajectory planning algorithms: A general overview. *Motion and Operation Planning of Robotic Systems*, 29(2015), (2015), 3–27.

[17] Maghdid, H. S., Lami, I. A., Ghafoor, K. Z., and Lloret, J. Seamless outdoors-indoors localization solutions on smartphones: implementation and challenges. *ACM Computing Surveys (CSUR)*, 48(4), (2016), 53.

[18] Obeidat, H., Shuaieb, W., Obeidat, O., and Abd-Alhameed, R. A review of indoor localization techniques and wireless technologies. *Wireless Personal Communications*, (2021).

[19] Simões, W.C., Machado, G.S., Sales, A.M., de Lucena, M.M., and Jazdi, N., de Lucena, V.F., Jr. A review of technologies and techniques for indoor navigation systems for the visually impaired. *Sensors*, (2020).

[20] Saeed, N., Nam, H., Al-Naffouri, T. Y., and Alouini, M. A state-of-the-art survey on multidimensional scaling-based localization techniques. *IEEE Communications Surveys & Tutorials*, 21(4), (2019), 3565-3583.

[21] Nessa, A., Adhikari, B., Hussain, F., and Fernando, X. N. A survey of machine learning for indoor positioning. *IEEE Access*, 8, (2020), 214945-214965.

[22] Ferreira, A., Fernandes, D., Catarino, A., and Monteiro, J. Localization and Positioning Systems for Emergency Responders: a Survey. *IEEE Communications Surveys & Tutorials*, (2017).

[23] Gamal, A., Saleh, M., and Elmahallawy, A. De-Noising of Secured Stego-Images using AES for Various Noise Types. Przeglad Elektrotechniczny, 2(2), (2023), 21-26.

[24] Sun, M., Wang, Y., Xu, S., Qi, H., and Hu, X. Indoor positioning tightly coupled Wi-Fi FTM ranging and PDR based on the extended Kalman filter for smartphones. *IEEE Access*, (2020).

[25] Wang, X., Qin, D., Guo, R., Zhao, M., Ma, L., and Berhane, T.M. The technology of crowd-sourcing landmarks-assisted smartphone in indoor localization. *IEEE Access*, (2020).

[26] Ibnatta, Y., Khaldoun, M., and Sadik, M. Exposure and evaluation of different indoor localization systems. In Proceedings of the 6th International Congress on Information and Communication Technology (pp. 731-742). Singapore: Springer, (2022).

[27] Kriz, P., Maly, F., and Kozel, T. Improving Indoor Localization Using Bluetooth Low Energy Beacons. *Mobile Information Systems*, (2016).

[28] Wang, C., Xu, A., Kuang, J., Sui, X., Hao, Y., and Niu, X. A high-accuracy indoor localization system and applications based on tightly coupled UWB/INS/floor map integration. *IEEE Sensors Journal*, 21, (2021), 18166–18177.

[29] Ibnatta, Y., Khaldoun, M., and Sadik, M. Indoor localization techniques based on UWB technology. In Proceedings of the International Symposium on Ubiquitous Networks (pp. 3-15). Cham, Switzerland: Springer, (2021).

[30] Labinghisa, B.A., and Lee, D.M. Indoor localization system using deep learning-based scene recognition. *Multimedia Tools and Applications*, (2022).

[31] Fiyad, H., Gamal, A., Mostafa, M., Zaghloul, A., Naser, M., et al. An improved real visual tracking system using particle filter. Przeglad Electrotechniczny, 11(1), (2021), 164–169.

[32] Shawky, H., Gamal, A., and Salem, A. S-Box Modification for the Block Cipher Algorithms. *Przeglad Electrotechniczny*, 2(4), (2023), 278–281.

[33] Masood, H., Zafar, A., Ali, M. U., Khan, M. A., Ahmed, S., et al. Recognition and tracking of objects in a clustered remote scene environment. *Computers, Materials & Continua*, 70(1), (2022), 1699–1719.

[34] Wang, X., Gao, L., Mao, S., and Pandey, S. CSI-based fingerprinting for indoor localization: A deep learning approach. *IEEE Transactions on Vehicular Technology*, 66(1), (2017), 763–776.

[35] Karamat, T. B., Lins, R. G., Givigi, S. N., and Noureldin, A. Novel EKF-Based Vision/Inertial System Integration for Improved Navigation. *IEEE Transactions on Instrumentation and Measurement*, 32(99), (2017), 1-10.

[36] Jang, B., and Kim, H. Indoor positioning technologies without fingerprinting map: A survey. *IEEE Communications Surveys & Tutorials*, 21(1), (2019), 508-525.

[37] Achroufene, A., Amirat, Y., and Chibani, A. RSS-based indoor localization using belief function theory. *IEEE Transactions on Automation Science and Engineering*, 16(3), (2019), 1163-1180.

[38] Scannapieco, A. F., Renga, A., Fasano, G., and Moccia, A. Ultralight radar sensor for autonomous operations by micro-UAS. In International Conference on Unmanned Aircraft Systems (ICUAS) (pp. 727–735), (2016).

[39] Dožić, S., Jovanović, M., Stojanović, I., and Dordević, G. L. Experimental evaluation of machine learning algorithms for fingerprinting indoor localization. *Facta Universitatis: Automatic Control and*

Robotics, 20(3), (2021), 179-188.

[40] Karunanithy, K., and Velusamy, B. Directional antenna based node localization and reliable data collection mechanism using local sink for wireless sensor networks. *Journal of Industrial Information Integration*, 24(1), (2021).

Authors Biography

Dr. Ahmed Gamal Abdellatif Ibrahim is a dedicated lecturer in the Department of Communications and Electronics Engineering at the Air Defense College in Alexandria, Egypt. He was born in 1985 in Sharkia Governorate, Egypt. In 2007, Dr. Gamal graduated with a B.Sc. degree with honors in Electronics and Electrical Engineering from the Air Defense College at Alexandria University. He continued his academic journey and obtained a master's degree in Electronics and Electrical Engineering from Alexandria University in 2017. Dr. Gamal has also demonstrated his commitment to expanding his knowledge and gaining international experience. In 2019, he became a Ph.D. student visitor at the prestigious Research Center of Geomatics (CIRGEO) at the University of Padua in Italy. This valuable experience allowed him to broaden his horizons and enrich his research pursuits. Dr. Gamal successfully completed his Ph.D. degree in Electronics and Communications Engineering in 2022. His research interests reflect his diverse background and multidisciplinary approach, including navigation, indoor positioning, tracking, filtering, information security, and image processing. Finally, He was a reviewer for several journals and major conferences.

Dr. Amgad Adel Salama received the B.Sc. and the M.Sc. degrees from Alexandria University, Alexandria, Egypt, in 2005 and 2012, respectively, and the Ph.D. degree from Concordia University, Montreal, QC, Canada, in 2017, all in electrical engineering. He is currently with the Egyptian research and development center, Cairo, Egypt. His research interests include sensor array signal processing, machine learning (deep learning), direction of arrival estimation, and beam forming. He was a reviewer for several journals and major conferences.

Hamed S. Zied is a teacher at Air Defense College, Alexandria, Egypt, and became a Member of IEEE in 2012. He was born in Minoufia, Egypt in 1973. He holds B.Sc. in Electronics and Communications from the Faculty of Engineering, Alexandria University; He also holds an M.Sc. and Ph.D. in Electrical Engineering from the Faculty of Engineering, Alexandria University. He taught many technical courses in Electrical and Electronic (Analog and Digital) system design and Implementation, and works as System Engineer for more than 15 years.

Dr. Adham Ahmed Elmahallawy is a highly qualified lecturer with a strong background in Communications, Electronics, and Electro Physics Engineering. He earned his Bachelor's degree with distinction and honors from Alexandria University in 1994. He has also completed several technical courses in electronic and communications engineering design and implementation. In 2001, Dr. Elmahallawy obtained his Master's degree in Electrical Engineering from Alexandria University. He went on to pursue his Doctor of Philosophy degree in electrical engineering, which he earned from the Department of Electronics and Communications Engineering at the University of Alexandria in 2010. Also, he has published different research papers in highly-rated journals. He currently serves as a lecturer at the Higher Institute of Engineering and Technology, King Mariout, Alexandria, Egypt.

Mahmoud A. Shawky was born in 1990 in Saudi-Arabia. He received his B.Sc. degree in Electronics and Electrical Engineering in 2012 from Air Defence College, Alexandria University, M.Sc. (Eng.) degree in Authentication Mechanisms in Computer Network Protocols from Alexandria University, Alexandria, Egypt. He is currently a lecturer in the Egyptian Air Defence College. He is currently pursuing a Ph.D. degree in James Watt School of Engineering, University of Glasgow, UK. His research interests are in the area of cryptography and number theory, digital signatures, authentication in wireless communications and cyber security.

Declaration of interests

☒ The authors declare that they have no known competing financial interests or personal relationships that could have appeared to influence the work reported in this paper.

☐ The authors declare the following financial interests/personal relationships which may be considered as potential competing interests: